NASA Contractor Report 3852

Toughening Mechanism in Elastomer-Modified Epoxy Resins–Part 2

A. F. Yee and R. A. Pearson

CONTRACT NAS1-16132
DECEMBER 1984

NASA

NASA Contractor Report 3852

Toughening Mechanism in Elastomer-Modified Epoxy Resins–Part 2

A. F. Yee and R. A. Pearson
General Electric Company
Schenectady, New York

Prepared for
Langley Research Center
under Contract NAS1-16132

National Aeronautics
and Space Administration

**Scientific and Technical
Information Branch**

1984

TABLE OF CONTENTS

LIST OF ILLUSTRATIONS

LIST OF TABLES

SUMMARY

The role of matrix ductility on the toughenability and toughening mechanism of elastomer-modified DGEBA epoxies was investigated. Matrix ductility was varied by using epoxide resins of varying epoxide monomer molecular weights. These epoxide resins were cured using 4,4' diaminodiphenyl sulfone (DDS) and, in some cases, modified with 10% HYCAR^{R} CTBN 1300X8. Fracture toughness values for the neat epoxies were found to be almost independent on the monomer molecular weight of the epoxide resin used. However, it was found that the fracture toughness of the elastomer-modified epoxies was very dependent upon the epoxide monomer molecular weight. Tensile dilatometry indicated that the toughening mechanism, when present, is similar to the mechanism found for the piperidine cured epoxies in Part 1.[1] SEM and OM corroborate this finding.

Dynamic mechanical studies were conducted to shed light on the toughenability of the epoxies. The time-dependent small strain behavior of these epoxies were separated into their bulk and shear components. The time-dependent small strain behavior of these epoxies were separated into the bulk and shear components. The bulk component is related to brittle fracture, whereas, the shear component is related to yielding. It can be shown that the rates of shear and bulk strain energy build-up, for a given stress are uniquely determined by the values of Poisson's ratio, ν. It was found that ν^* increases as the monomer molecular weight of the epoxide resin used increases. This increase in ν^* can be associated with the low temperature β relaxation. The effect of increasing cross-link density is to shift the β relaxation to higher temperatures and to decrease the magnitude of the β relaxation. Thus, increasing cross-link density decreases ν^* and increases the tendency towards

brittle fracture. The nature and origin of the low temperature relaxation peaks is briefly addressed.

1. INTRODUCTION

In our previous work (Part 1)[1] the micromechanical mechanisms that contribute to the toughness of elastomer-modified epoxies were investigated. For a range of rubber particles from 0.1 to 10 μm in diameter, the deformation mechanisms were found to be qualitatively similar. Furthermore, we deduced that the role of the rubber particles in toughened epoxies was to cavitate dissipating the bulk strain energy in the matrix and, in turn, promoting the formation of shear bands in the matrix. Together, these two processes produce a plastic zone ahead of the crack tip, which effectively blunts the sharp crack and results in increased toughness. This deduction is in agreement with those reached by Bascom and coworkers[2,3] and is qualitatively similar to the toughening mechanism in thermoplastics which do not readily craze.

However, not all epoxy resins can be toughened by elastomeric modification. Meeks[4] has shown that the toughness enhancement obtained by elastomeric modification of epoxy resins is dependent on the structure of the curing agent. This dependence may actually reflect varying degrees of cross-link density. Several others[5-8] have come to similar conclusions: that the fracture toughness of neat epoxies decreases as cross-link density increases. High cross-link density has been cited as the reason for the lack of toughness enhancement in some elastomer-modified epoxies.[6]

Since in our previous work we have identified the matrix as the major energy absorbing component, it stands to reason that modifying the matrix may lead to enhanced toughness. More specifically, the ability of the matrix to form shear bands should be directly related to the amount of energy it can dissipate, i.e., matrix toughenability. Furthermore, since ductility requires

large scale cooperative conformational rearrangements of the polymeric backbone, it is reasonable to expect that the reduction of cross-link density should result in increased ductility. Consequently, the elastomer-modified ductile epoxy can be expected to exhibit enhanced toughness.

The purpose of this work is to investigate the role of the matrix in the deformation mechanisms of these complex materials. The use of trademarks or names of manufacturers in this report does not constitute endorsement, either expressed or implied, by the National Aeronautics and Space Administration.

2. EXPERIMENTAL APPROACH

In order to investigate the role of matrix ductility on the toughenability of DGEBA epoxy resins, several plaques of varying cross-link densities were produced. The control of cross-link density of these resins was obtained by curing epoxide resins of varying molecular weights. ^{13}C NMR was performed on the epoxy monomers to experimentally determine their average monomer molecular weights. Differential Scanning Calorimetry, using a Perkin-Elmer DSC-IIA and scanning at a rate of 10°C/min on ca. 10 mg samples, was performed to determine the glass transition temperature of the cured epoxy plaques. The glass transition temperature provided a qualitative assessment of cross-link density.

In principle, the molecular weight between cross-links may be determined using an equation from the theory of rubber-elasticity:[9]

$$G_e = g \left(\frac{r_e^2}{r_o^2}\right) \nu R T \qquad (1)$$

where G_e is the equilibrium shear modulus in the rubbery region.

ν is the cross-link density,

R is the gas constant,

T is the absolute temperature,

g is a numerical factor approximately equal to 1,

r_e^2 is the mean square end-to-end distance of the strands which are cross-linked,

r_o^2 is the mean square end-to-end distance that the same strands would assume if they are not cross-linked.

Since $v = \rho / \overline{M}_{nc}$, where ρ is density and $\overline{M}_{nc}$ is the number-average molecular weight between cross-links, then $\overline{M}_{nc}$ can be easily determined from dynamic mechanical data using the following equation, assuming g=1 and $\frac{r_e^2}{r_o^2} = 1$:

$$\overline{M}_{nc} = \frac{\rho RT}{G_e} \tag{2}$$

The dynamic mechanical data were obtained with a Rheometrics Mechanical Spectrometer equipped with a torsional fixture for solids. Shear moduli were measured under oscillating torsion at 1Hz with strain amplitudes of 0.4 - 1.6%. Samples were heated in a nitrogen atmosphere in five-degree steps with a five-minute dwell time, at the end of which G', G" and Tan δ were determined. The value, P, was estimated to be 1.2 g/cm^2 from values given in Table 3.1.

The fracture toughness of several neat resins and elastomer-modified resins were measured in terms of the critical strain energy release rate G_{1c}, which was determined using single-edge notched specimens (approximately 63.5mm L x 12.7mm W x 6.1mm T) fractured in three-point bending with a span of 50.8mm. G_{Ic} was calculated using the following relationship[10,11]

$$U = G_{Ic}\, B\, D\, \Psi \tag{3}$$

where U is the stored elastic energy,

B is the specimen thickness,

D is the specimen width,

Ψ is a function relating the change in compliance with crack length.

For each material, at least six SEN specimens with varying crack lengths were fractured on a screw driven Instron (Model 1125) at a rate of 2.12 mm/s.

A Nicolet 2090 digital oscilloscope captured the load vs. time trace. The average crack length of each specimen was measured using an optical microscope. An HP-86 desktop computer was programmed to integrate the load vs. time trace. In this manner, the energy absorbed was calculated and, together with the measured crack lengths, the G_{Ic} was determined.

Deformation mechanisms were determined by a tensile dilatometry technique modeled after that used by Bucknall[12], except that a constant displacement rate was used. Details of this technique were given in Part 1.[1] The deformation mechanism of a material could then be ascertained by analyzing the volume strain vs. elongational strain plot. In such plots, initially one typically sees an increase in volume strain due to the Poisson's effect; thereafter, deformational processes such as voiding result in a further increase in the volume strain, whereas shear deformation results in a decrease in the volume strain. This decrease is an artifact of the technique and not necessarily real but it is very useful for signaling the onset of shear banding processes (see Part 1).[1]

To complement the volume strain data, fractography was performed on the SEN fracture toughness specimens. This involved the analysis of the fracture surface via Scanning Electron Microscopy and of the subsurface damage via Transmission Optical Microscopy. The major tool for SEM analysis was an ISI Super II Scanning Electron Microscope. SEM specimens were coated with a thin film of Au-Pd by sputtering. A Zeiss optical microscope was used to examine thin sections of material removed from planes perpendicular to the fracture surface. These thin sections of film were prepared by potting fractured specimens in epoxy followed by thinning down with a polishing wheel. Details of these techniques were given in Part 1.[1]

3. MATERIALS

The materials used in this investigation consisted of several DGEBA epoxide resins of varying epoxide equivalent weights from Dow Chemical Company, cured with stoichiometric amounts of 4,4'-diaminodiphenyl sulfone (DDS) from the RSA Corp. The manufacturers data of the DGEBA epoxide resins are given in Table 3-1. These same resins were also modified with Hycar CTBN 1300x13, a liquid copolymer of butadiene and acrylonitrile terminated with carboxyl end groups kindly supplied by the B.F. Goodrich Chemical Company. All materials were used as received. Hycar CTBN 1300x13 was chosen as the elastomer modifier since it resulted in the formation of 1-10μm rubber particles upon curing. Specific formulations used in this investigation are presented in Table 3-2.

The number of DGEBA repeat units, n, (see Figure 3-1), for the epoxide monomers was determined using ^{13}C NMR. The ratio of the area of the signal from tertiary carbon on the BPA unit versus the half area of one of the epoxide carbon signals indicated the ratio of BPA units with respect to the two epoxide groups. Subtracting one from this ratio gives n. Table 3-3 compares values of n calculated from manufacturer's data with the values of n deforming using ^{13}C NMR. The large discrepancy in n for the DER664 resin leads us to the conclusion that the monomer molecular weight was greater than that specified by the manufacturer and may account for excess DDS seen in our cured plaques.

Epoxy plaques were prepared as follows: The epoxide resin was placed in a glass mixing jar. If a solid resin was used, the jar with the resin was placed in an oven at a temperature sufficiently high to melt and consolidate the resin. For those specimens that were elastomer-modified, ten volume per-

cent of the CTBN was added. Then a stoichiometric amount of DDS was added. This jar was immersed in a silicone bath for about 45-60 min. at ca. 20°C above the typical cure temperature. This mixture was then mechanically stirred for ca. 30 min. to dissolve the DDS, then degassed. The mixture was poured into a mold that had been preheated at the cure temperature and cured using one of three cure schedules.

The curing schedule depends upon the molecular weight of the epoxide monomers which possessed widely varying viscosities. These viscosities were determined using a Rheometrics Mechanical Spectrometer. Figure 3.2 is a plot of viscosity vs. temperature for several solid DGEBA epoxide resins. Since these resins were poured into a Teflon-coated* mold, it was advantageous for the viscosity of these resins to be less than 100 poise, which occurred at about 20-25°C above the melting points for each of these resins. With this information the following three cure schedules were employed:

RESIN		FIRST CURE	POST CURE
DER332	337	120°C for 16 hours	200°C for 2 hours
DER661	662	140°C for 16 hours	200°C for 2 hours
DER664	667	160°C for 16 hours	200°C for 2 hours

These curing schedules are modifications of those published by Lee and Neville.[13] A 250°C post cure was required for DER332 since its T_g was greater than 200°C.

* Teflon is a registered trademark of E.I. duPont and Company.

TABLE 3-1

Commercial Data Of Epoxy Resins Given By Dow Chemical Company

DGEBA Resin	Epoxide Equivalent Weight	n*	Viscosity (Duran's Mp°C)	SpG (g/ml)
DER332	172-176(174)	0	40-50 poise	1.16
DER337	230-250(240)	0.42	viscous	1.16
DER661	475-575(525)	2.2	70-80°C	1.18
DER662	575-700(638)	3.0	80-90°C	1.18
DER664	875-975(925)	4.8	95-105°C	1.18
DER667	1600-2000(1800)	10	115-130°C	1.18

* n calculated by $n = \frac{MW-348}{315}$

TABLE 3-2

Epoxy Formulations Used In This Investigation

Resin	n	Mass Resin (g)	Mass DDS (g)	When Modified Mass CTBN (g)
DER332	0	500	189.3	60.3
DER337	.42	500	133.3	56.3
DER332/661	1.0	43.3/406.7	89.3	51.8
DER661	2.2	500	61.0	49.9
DER662	3.0	300	50.0	49.1
DER664	4.8	500	34.6	47.9
DER667	10	500	17.8	46.6

TABLE 3-3

A Comparison Of Calculated Values of n
(n= The Number of DGEBA Repeat Units)
for Epoxy Monomers

Resin	n Calc. From Avg. Monomer Molecular Weights	n Determined by ^{13}C NMR
332	0	0
661	2.2	2.8
664	4.8	5.7
667	10.2	10.6

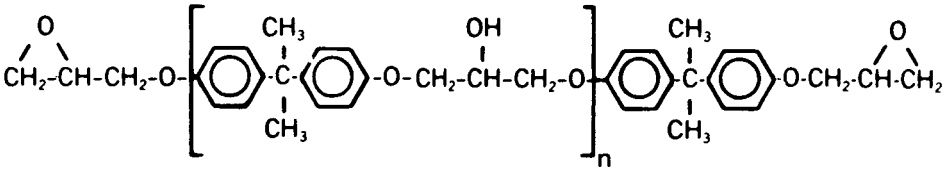

Figure 3-1. A schematic of the general chemical structure of the DGEBA epoxide monomers used in this investigation.

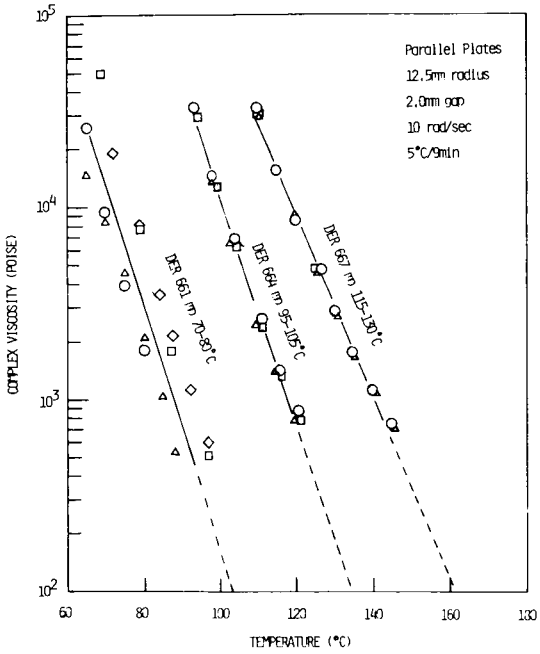

Figure 3-2. The effect of temperature on the complex viscosity on several solid epoxide resins used to determine cure temperatures.

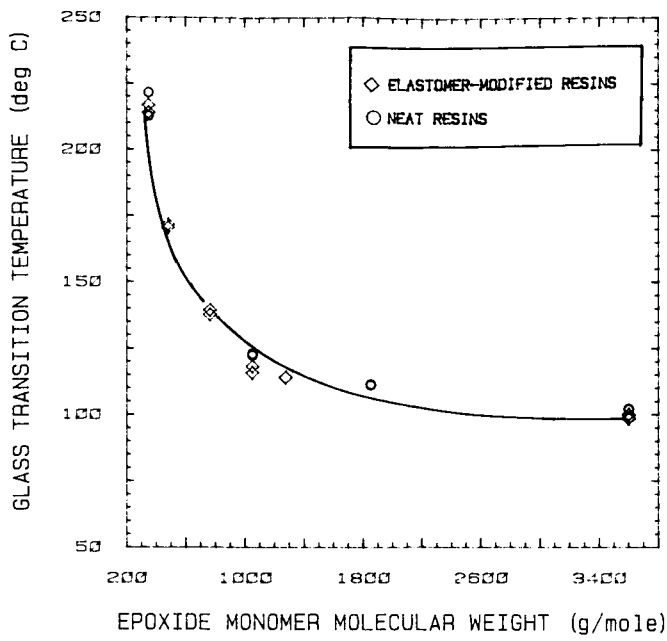

Figure 3-3. The effect of monomer molecular weight on the glass transition temperatures of several DGEBA epoxies.

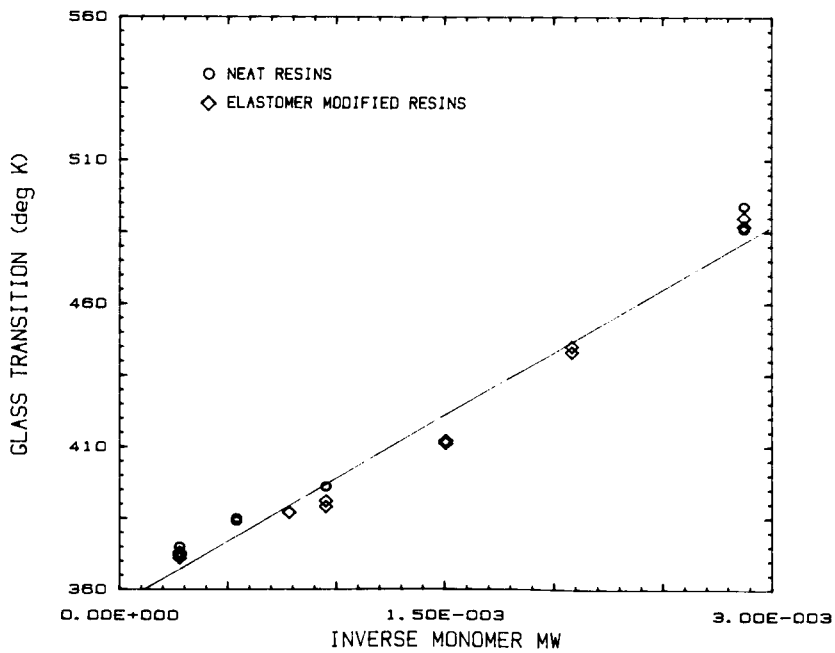

Figure 3-4. The glass transition temperature versus inverse epoxide monomer molecular weight that suggests a linear relationship.

4. CROSS-LINK DENSITY DETERMINATIONS

In a series of various monomer molecular weight epoxide resins cured with the same curing agent, the glass transition temperature is a qualitative measurement of the cross-link density, i.e., the higher the cross-link density the greater the glass transition temperature. The glass transition temperatures of cured epoxy plaques were determined by DSC; the results are plotted against molecular weight between cross-links in Figure 4-1. It is interesting to note that the T_g initially decreases rapidly as the monomer molecular weight of the epoxide resin is increased (220°C to 120°C), but, at monomer molecular weights greater than 1080 g/mole, the T_g only slightly decreases as the molecular weight between cross-links is increased. A close examination of the literature reveals that several attempts have been made to relate the glass transition temperature to the cross-link density or the number average monomer molecular weight between cross-links. Only two empirical approaches are included in the following discussion.

The number average molecular weight between cross-links ($\overline{M}_c$) has been empirically related to T_g by Nielson.[14] He suggests that $\overline{M}_c$ can be roughly estimated by the use of the following relationship:

$$T_g - T_{g_o} = \frac{3.9 \times 10^4}{\overline{M}_c} \qquad (4)$$

where T_{g_o} is the glass transition temperature of the uncross-linked polymer. Nielson cautions that this equation only accounts for the effect of cross-link restrictions on molecular motion and not for the so-called copolymer effect. In the present case, our T_g data for the solid resin DER667 was found to be lower than the melting point, which indicates that there may be some crystal-

linity in the solid. This results in a negative $T_g - T_{g_o}$ value of the uncross-linked DER667 resin. Consequently, this approach to relating cross-link density to the glass transition temperature was abandoned.

Ellis and Banks[15] have used an empirical fit to the glass transition temperature vs. the monomer molecular weight data for highly cross-linked DGEBA epoxies with remarkable success. The following equation was used:

$$T_g = A + B \overline{M}_n^{-1} \tag{5}$$

where A and B are constants. A is related to the T_g of an infinitely linear polymer with the same repeat unit as the epoxies (The T_g of phenoxy resin is 373°C). B may be related to the T_g of a highly cross-linked polymer composed solely of the tetrafunctional cross-linking agent. A polymer of this type may degrade before ever reaching its T_g. This relationship is of a very general form and has been used by Rietsch[16] to predict the effect of MW on the T_g of linear and cross-linked polystyrenes.

Ellis and Banks[15] used a least squares fit of the glass transition temperatures of several DGEBA resins cured with DDM (diaminodiphenyl methane) to the inverse of the monomer molecular weight and determined that A=365 and B=17300. Following this procedure, the glass transition temperature is plotted against the inverse monomer molecular weight for DGEBA resins cured with DDS (Figure 4-2). The least-squares fit gives A=354 and B=44000. The reason for B being larger for the DDS cured DGEBA resins than the DDM cured resin may be that DDS is a more rigid molecule.

As discussed previously in the experimental section, the molecular weight between cross-links may be determined from the theory of rubber-elasticity. This theory relates the equlibrium shear modulus to the molecular weight

between cross-links (see Equation 2). Figure 4-3 is a plot of the storage shear moduli versus temperature for four DDS cured DGEBA epoxide resins of varying monomer molecular weight. The equilibrium shear modulus is taken to be the value at a temperature above T_g and well into the rubber plateau where it approaches a constant. This typically occurs at 50 degrees above T_g . The number average molecular weights between cross-links calculated using Equations 1 and 2 are tabulated in Table 4-1. Note that density = 1.2 g/cm^3 , g=1 and $\frac{r_1^2}{r_o^2}$ =1 were used in these calculations. The number-average molecular weights between cross-links are calculated using the following equations:

$$\overline{M}_{nc} = \frac{2M_e + M_d}{3}$$

where M_e is the epoxide monomer molecular weight and,

M_d is the molecular weight of DDS (256 g/mole)

It is important to note that the molecular weight between cross-links increases as the molecular weight of the epoxy monomer is increased. However, the experimentally determined number-average molecular weight between cross-links, $\overline{M}_{nc}$, are much higher than the values predicted from ideal stoichiometric reactions. One reason for the greater $\overline{M}_c$ may be the presence of ether linkages, as Ochi et al.[17] proposes. However, the preponderance of evidence[15,18,19] points to etherification as a very minor reaction when primary amine curing agents are used.

Takahama and Geil[20] attributed the differences between predicted cross-link densities and experimentally determined cross-link densities using the rubber-plateau modulus to changes in the apparent front factor $(\frac{r_1^2}{r_o^2})$. These

authors found the same trend as that observed in this work, viz., as the cross-link density decreased, the measured cross-link density deviated systematically by larger amounts from prediction. They reconciled this discrepancy by assuming that the apparent front factor changed from 0.84 to 0.24. They, however, did point out that rubberlike-elasticity theory may not be appropriate for the difunctional anhydride cured system used in their work. Katz and Tobolsky[21] have reported a front factor ranging from 0.78 to 1.62 for several amine cured epoxies. However, in both cases the front factors were not experimentally determined. In our calculation, we made no attempt to vary the apparent front factor in order to obtain better agreement between the experimental and the calculated results.

TABLE 4-1

Molecular Weight Between Cross-Links

Resin	Monomer Molecular Weight (g/mole)	G_e (dyne/cm^2)	T (°K)	$\overline{M}_{nc}$ calc. from G_e (g/mole)	$\overline{M}_{nc}$ calc. from m.w. (g/mole)
DER332/DDS	334-352	1.3×10^8	546	420	317
DER661/DDS	950-1150	2.8×10^7	443	1600	785
DER664/DDS	1750-1950	1.97×10^7	428	2200	1319
DER667/DDS	3200-4000	7.0×10^6	423	6000	2485

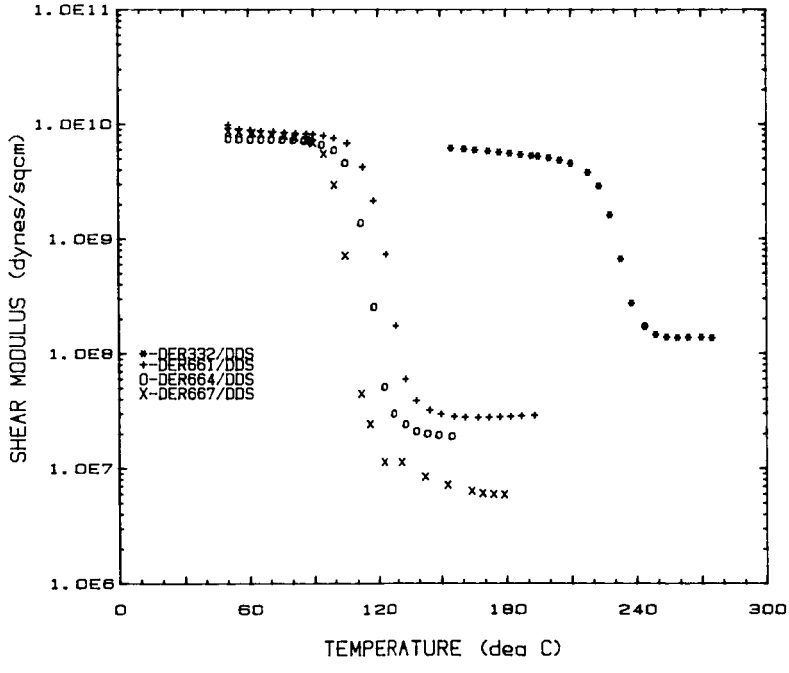

Figure 4-1. Shear modulus versus temperature measured in torsion to determine the molecular weight between cross-links.

5. FRACTURE TOUGHNESS RESULTS AND DISCUSSION

The energy per unit cross-sectional area (U/BD) for SEN specimens of varying crack lengths for each material were plotted vs. $\Phi = dc/da$ and the data were fitted to a linear curve by the method of least-squares. The slope of this line is equal to the G_{Ic} of the material. Figure 5-1 is a plot of U/BD vs. Φ for three lots of DER667/DDS/13(10%). Figure 5-2 illustrates the large differences in the slopes (G_{Ic}'s) of the elastomer modified resins. Figure 5-3 is a plot of G_{Ic} versus the epoxide monomer molecular weight for the neat resins as well as the elastomer modified resins. These results show that the inherent fracture toughness of the neat resins increases slightly as the monomer molecular weight increases, while in the rubber-modified series almost two orders of magnitude increase was seen. The neat epoxy resins have G_{Ic} values that are in the same range as those reported by Scott, et al.[7] on aliphatic amine cured epoxies and by Cherry and Thompson[8]. In contrast, the fracture toughness of the elastomer-modified epoxies is strongly dependent upon the molecular weight of the epoxide monomer. Therefore, the toughenability of a DGEBA epoxy by elastomer-addition depends upon the cross-link density of the epoxy matrix. The lower the cross-link density, the greater the toughenability. This reduction in cross-link density appears to be the reason for the toughness enhancement when BPA was added as a resin modifier in our previous investigation (Part 1). This effect was also observed by Riew et al.[22]

The toughening effect may be understood in terms of the size of the plastic zone which blunts the sharp crack. According to the Dugdale model[32], the size of the plastic zone is inversely proportional to the yield stress. Thus, any means that reduces the yield stress should result in an increased plastic

zone and higher toughness. In Table 5-1 we have tabulated the G_{Ic} , σ_y , calculated plastic zone ρ_{calc} and measured plastic zone $\rho_{measured}$. The calculated plastic zone ρ_{calc} is the effective crack tip radius calculated using $\rho_{calc} = G_{Ic} / \sigma_y$. The measured plastic zone $\rho_{measured}$ was determined using optical microscopy. The measured plastic zones tend to be larger than those calculated. Now the σ_y of these epoxies may be reduced by decreasing the cross-link density or by the addition of a rubber phase. However, the yield stresses of DER 667 and DER 661 modified with 10% elastomer only differ by ca. 10%, while their shear and tensile moduli (not shown) are comparable. Thus, the change in toughness cannot be accounted for by the lower yield stress alone. Clearly, an analysis of the micromechanical deformation is needed to understand the energy processes providing toughness enhancement.

TABLE 5-1

A Comparison Of Calculated And Measured Plastic Zones

Resin	G_{Ic} (J/m^2)	σ_y mPa	$\rho_{calc.}$ m x 10^{-6}	$\rho_{measured}$ m x 10^{-6}
332	162	--	--	--
661	201	96.1	2.1	--
667	326	85.6	3.8	--
332/(13%)	242	--	--	--
661/(13%)	3000	81.5	36	62
667/(13%)	11400	73.3	156	500

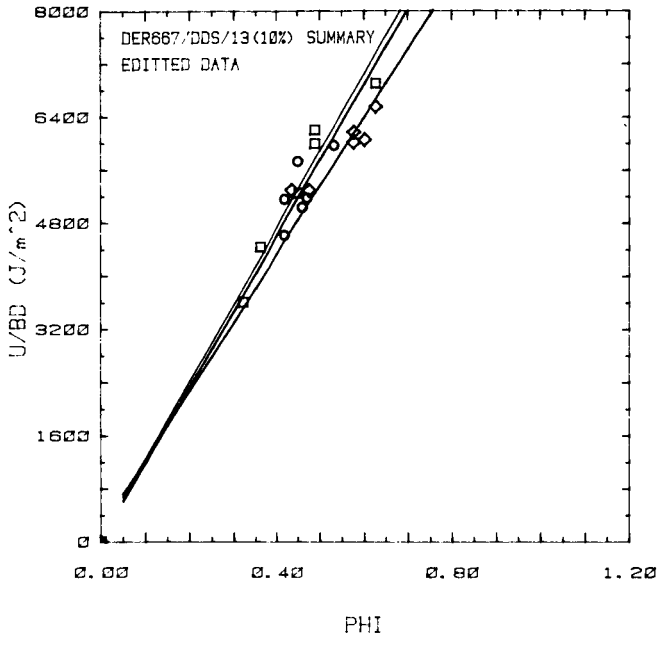

Figure 5-1. An illustrative plot of the data used to calculate the G_{Ic} of three plaques of DER667/DDS/CTBN(10%).

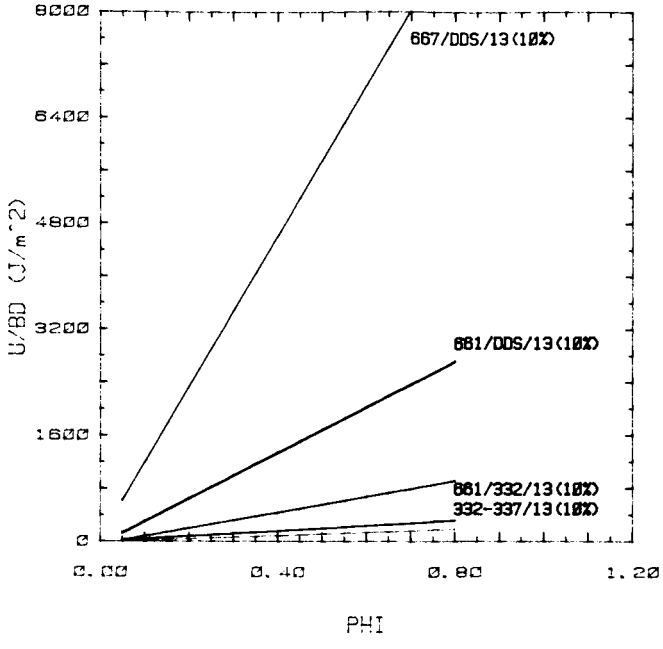

Figure 5-2. An illustrative plot of the magnitude of the slopes (G_{Ic}) determined in the fracture toughness measurements of this investigation.

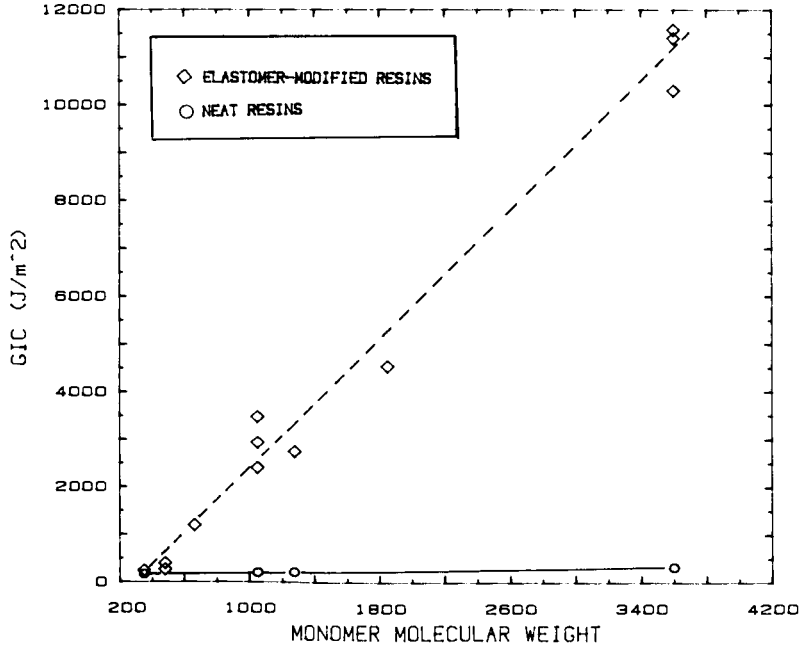

Figure 5-3. Fracture toughness G_{Ic} versus epoxide monomer molecular weight of the neat resins and elastomer modified resins.

6. VOLUME DILATION RESULTS AND DISCUSSION

Volume dilation techniques have been used to elucidate the toughening mechanisms in thermoplastics. Bucknall[12] has shown a large increase in volume strain when testing high impact polystyrene and concluded that crazing was the major energy dissipation mechanism. Hooley et al.[23] has shown that PMMA can be toughened by the addition of rubber. They used the volume strain technique to show that the slope of the volume strain curve decreased upon rubber modification. They interpreted these results to mean that a shear process is responsible for the toughening effect. Maxwell and Yee[24] used a volume dilation technique to determine that crazing was a major energy consuming mechanism in elastomer-modified polyphenylene oxide/polystyrene blends. Their TEM micrographs from deformed specimens provided conclusive evidence of crazing in these systems. This very same technique was used on piperidine-cured CTBN modified epoxies in our previous report.[1]

In this study, volume dilation experiments were again performed on two of the neat epoxies and their corresponding elastomer-modified versions to elucidate the toughening mechanism(s). These experiments also provided stress vs. strain data. In this investigation, only the results at 25.4mm/s crosshead rate will be examined since our previous work had shown that at this rate the deformation behavior of the neat and elastomer-modified epoxies are more clearly differentiated.

At a crosshead rate of 25.4 mm/s and at room temperature, dog bone specimens of DER332/DDS failed in a brittle matter. This material failed at less than 1% strain and did not exhibit a yield point. Brittle failure occurred even when the DER332/DDS epoxy was modified with 10% HYCAR CTBN 1300X8. The

volume strain increase seen in these materials was due solely to the Poisson's Effect and thus gave no insight into the deformation mechanism(s). However, as the cross-link density of these epoxies are reduced they do exhibit a yield point and the deformation mechanisms are discernable by volume strain measurements.

Figure 6-1 is a plot of stress and volume strain versus longitudinal strain for DER661/DDS and DER661/DDS/13(10%). Note that these materials exhibited yield, and, as expected, the incorporation of rubber inclusions decreased Young's Modulus and the yield stress. The volume strain curve for the neat resin indicates that this material deforms by a shear process. However, the corresponding curve for the elastomer modified material indicates that a volume increasing process is superimposed on the shear process. Based on our conclusions from Part 1, we can surmise that this volume increasing process is most likely voiding. Thus, the toughening mechanism for these epoxies is qualitatively similar to the piperidine cured epoxies studied in Part 1.

Figure 6-2 is a plot of stress and volume strain versus strain for the DER667/DDS materials, the lowest cross-link density epoxies studied in this investigation. The volume strain curve for the neat resins exhibited the now familiar shear behavior. The volume strain curve for the elastomer-modified version indicates that the voiding process is also present. These conclusions are supported by microscopy, which is described in the next section.

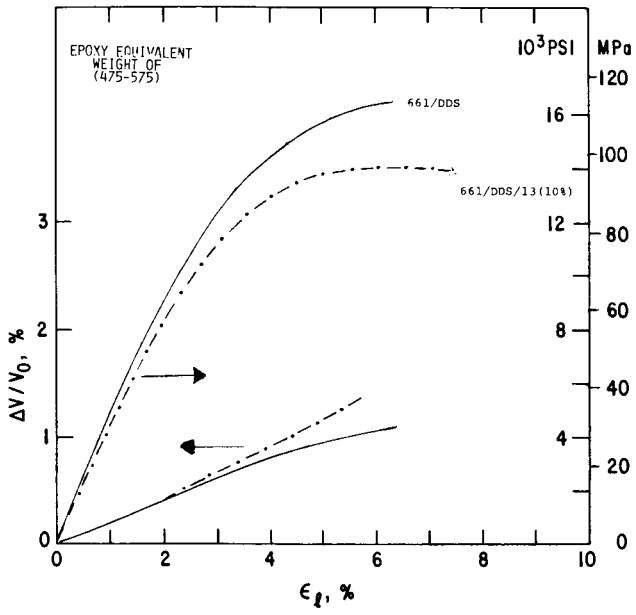

Figure 6-1. Tensile dilatometry results at a cross-head rate of 25.4 mm/s for the DER661/DDS epoxy and and the same epoxy modified with 10 vol% elastomer.

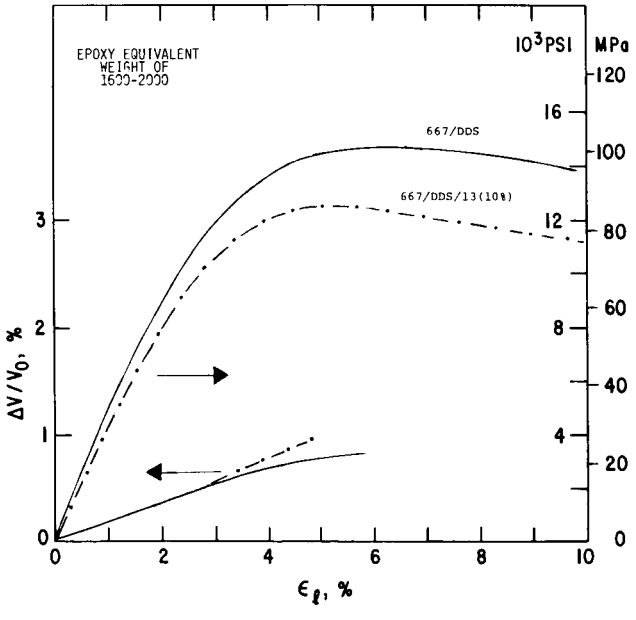

Figure 6-2. Tensile dilatometry results at a crosshead rate of 25.4 mm/s for the DER667/DDS epoxy and the same epoxy modified with 10 vol% elastomer.

7. MICROSCOPY

The SEM micrographs of the fracture surfaces of three SEN specimens of elastomer-modified epoxies of increasing monomer molecular weight (DER332, DER661 and DER667 respectively) are shown in Figures 7-1, 7-2 and 7-3. For the most highly cross-linked system (DER332), the fracture surface (see Figure 7-1) contains very shallow and nearly hemispherical voids. This SEM micrograph was taken at the region of the specimen where the starter crack had been arrested and then re-propagated during the three-point-bend test. This micrograph suggests that no plastic zone has been formed. The correlation between the lack of toughness and the lack of a significant plastic zone will be discussed in the conclusion section.

In Figure 7-2, the SEM micrograph of the fracture surface of the DER661-based epoxy, which is not as highly cross-linked as the DER332-based epoxy, shows that the void regions are comparatively less hemispherical and are deeper, which indicates that the rubber particles had cavitated and were then subjected to a shear deformation. Note that there is no evidence of debonding. This micrograph was taken in the region where the starter crack had stopped and a stress-whitened or plastic zone had formed prior to unstable fracture. The stress whitening results from the scattering of light by the voided rubber particles. The formation of this plastic zone correlates well with the toughening effect seen in this elastomer-modified epoxy.

The SEM micrograph (Figure 7-3) of the fracture surface of the elastomer-modified epoxy, DER667, which is the least cross-linked epoxy studied in this investigation, shows that the rubber particles have cavitated and been sheared more severely as one progresses from the starter crack region into the stress-

whitened region. The length of this zone extends from the area where the starter crack is arrested to the opposite edge of the SEN specimen. Also the sides of the specimen near the fracture are concave, indicating the onset of plane stress fracture, which is another sign that the material is indeed tougher. This material exhibited the largest plastic zone and the highest G_{Ic} .

The nature and extent of the sub-surface plastic zone formed ahead of the crack tip may be elucidated by using transmission optical microscopy. In our previous work (Part1)[1] we presented micrographs of the sub-surface plastic zone using bright field and cross-polarized light. The bright field imaging accentuates the cavitated rubber particles which, being efficient light scatterers, appear almost black. The crossed-polarized light renders visible the shear bands which are composed of more highly oriented material which is birefringent.

Figure 7-4 is an optical micrograph of the material beneath the fracture surface of the elastomer-modified DDS-cured DER332 epoxy. The examined section is rather thick (approximately 25μm) but still no voided (dark) rubber particles are evident. Upon close examination, one may observe a small plastic zone of about one rubber particle diameter in thickness just below the fracture surface.

Figure 7-5 is an optical micrograph of a sub-surface view of the less highly cross-linked elastomer modified DER661 SEN specimen. Even under crossed polarized light, the cavitated rubber particles of the plastic zone can be seen. A significant number of shear bands may be seen connecting these voided rubber particles. This region extends several tens of microns beneath the fracture surface.

Figure 7-6 is a optical micrograph of the toughest elastomer modified epoxy tested in this study DER667/005/13(10%). The size of the plastic zone is enormous. At this magnification, the entire zone cannot be contained in one micrograph. The size of the cavitated rubber particles are largest near the fracture surface. The number of shear bands is also very significant. Clearly, the formation of this plastic zone must have consumed a significant amount of energy which results in the high toughness.

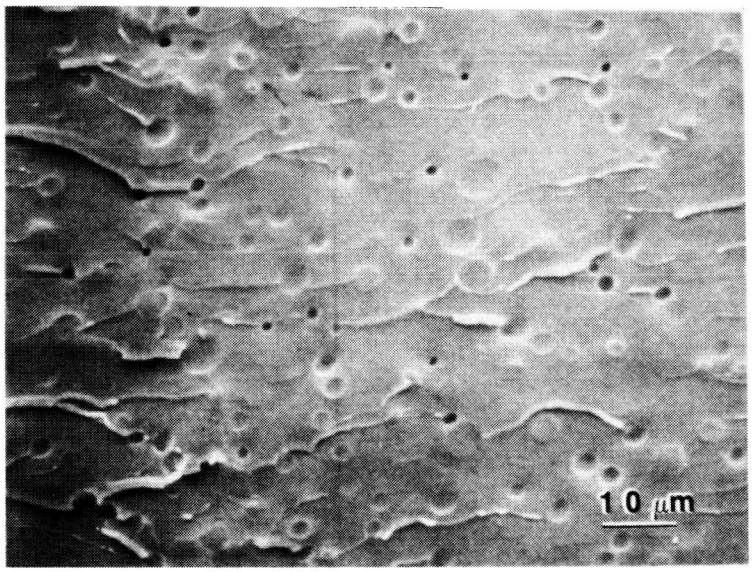

Figure 7-1. An SEM micrograph of the fracture surface of the 332/DDS/13(10%) SEM specimen taken at the region where the pre-crack had been re-propagated.

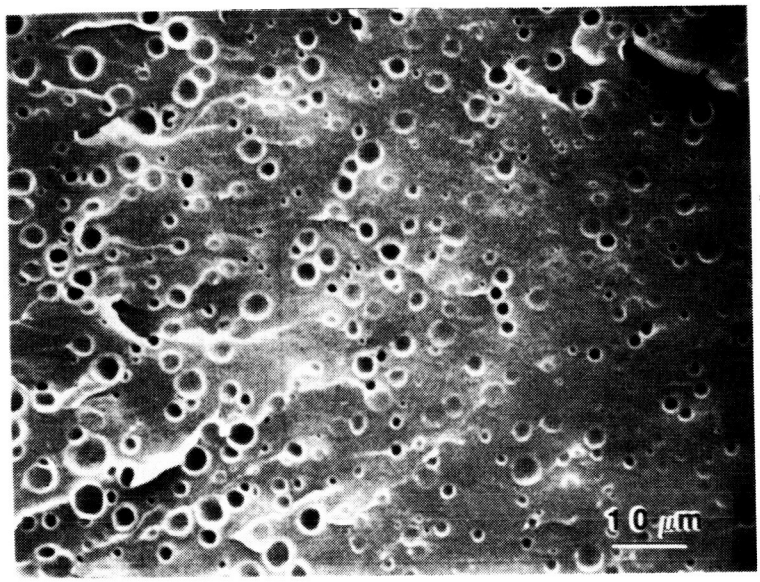

Figure 7-2. An SEM micrograph of the fracture surface of the 661/DDS/13(10%) SEM specimen taken at the region where the pre-crack had been re-propagated (the beginning of the plastic zone).

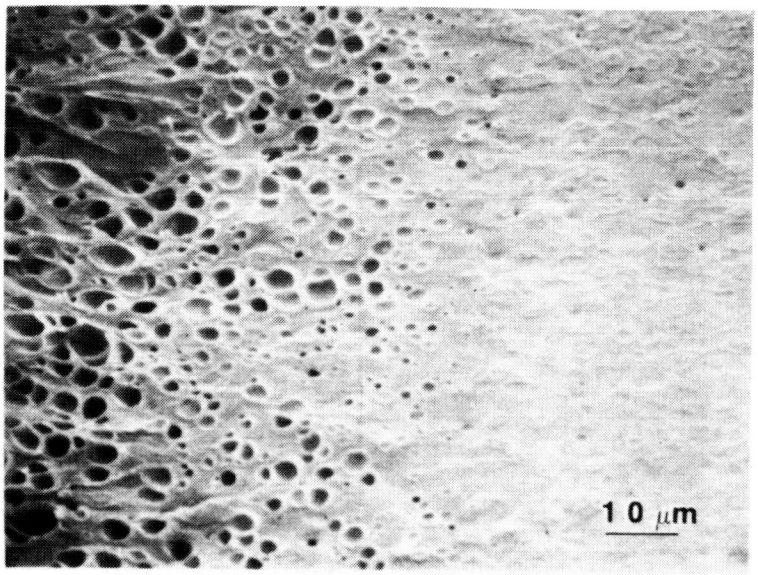

Figure 7-3. An SEM micrograph of the fracture surface of the 667/DDS/13(10%) SEM specimen taken at the region where the pre-crack had been re-propagated (the beginning of the plastic zone).

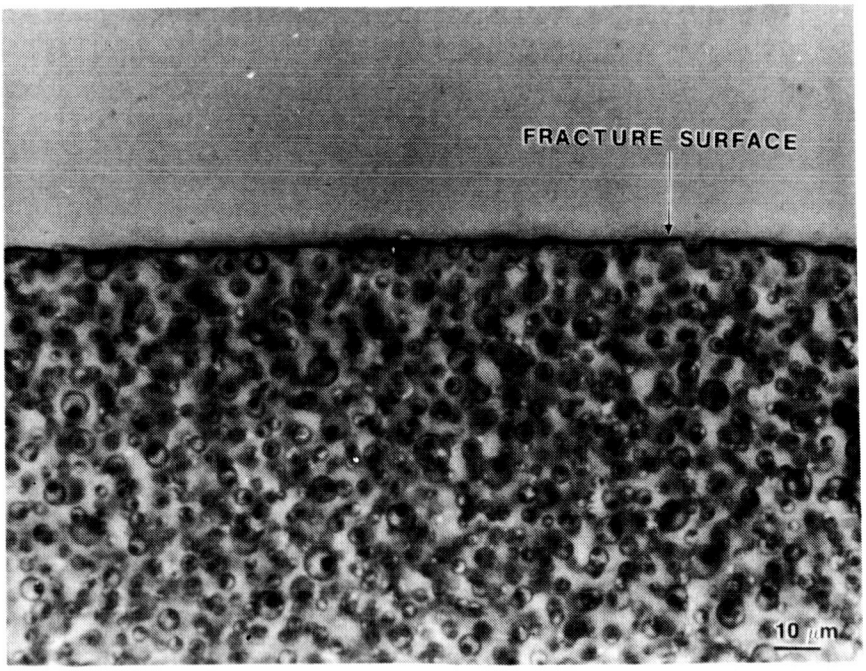

Figure 7-4. An optical micrograph, taken under cross-polarized light of the subsurface view of the plastic zone of a 332/DDS/13(10%) SEM specimen.

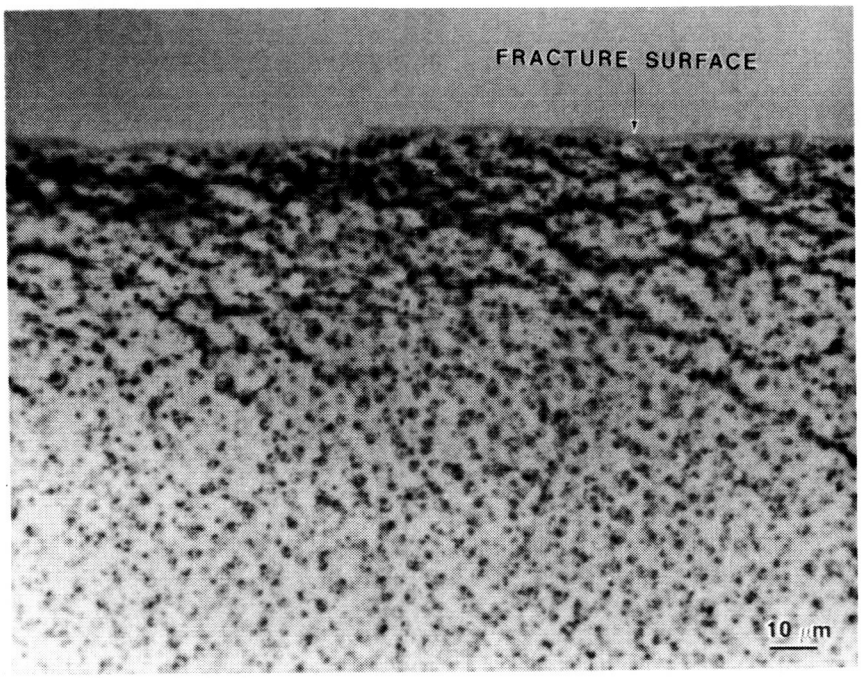

Figure 7-5. An optical micrograph, taken under cross-polarized light of the subsurface view of the plastic zone of a 661/DDS/13(10%) SEM specimen.

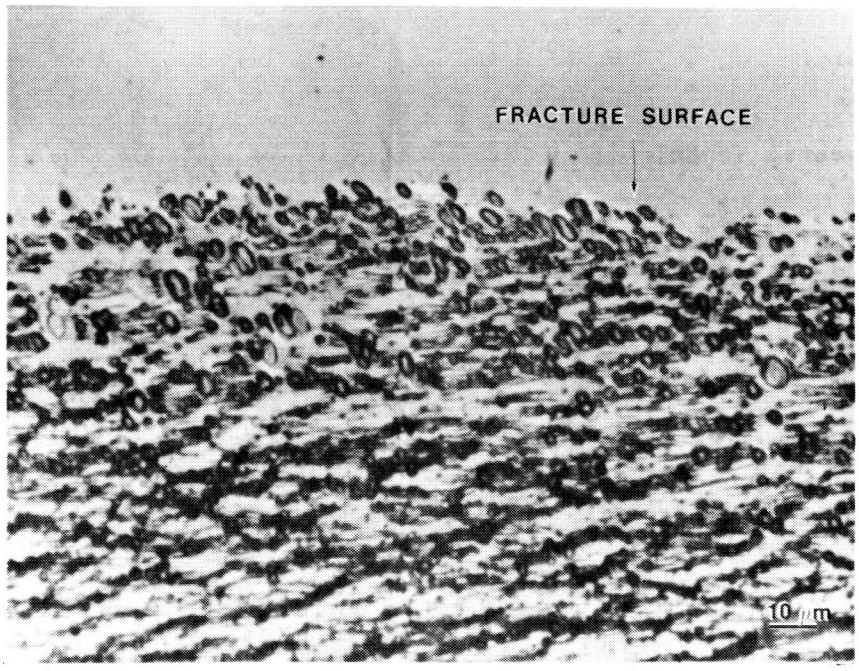

Figure 7-6. An optical micrograph, taken under cross-polarized light of the subsurface view of the plastic zone of a 667/DDS/13(10%) SEM specimen.

8. DYNAMIC MECHANICAL STUDIES

Dynamic mechanical studies were conducted to discover if in the neat resins correlations exist between the viscoelastic behavior and their large deformation behavior. In previous publications[25,26] we have pointed out that it is useful to separate the time-dependent small strain mechanical behavior of polymers into their bulk and shear components. We postulated that while the shear relaxation behavior is related to yielding its bulk counterpart is related to brittle fracture, because the former type of deformation involves shear flow whereas the latter dilatation.[26] In the present study, the toughness in elastomer-modified epoxies is found to be due mostly to the inherent ability of the matrix to deform by shear banding, the role of the elastomer particles being merely to reduce the constraints caused by the presence of a crack so that the inherent potential of the matrix to undergo shear flow can be unleashed. These findings are consistent with our thesis that studying the bulk and shear viscoelastic behavior of the epoxies can shed light on their toughenability.

8.1 Experimental Techniques

The dynamic bulk relaxation in a polymer is difficult to measure. However, by measuring the complex Young's modulus E*, and the complex Poisson's Ratio ν^*, the complex bulk and shear moduli, i.e., K* and G*, can be calculated by using the simple viscoelastic relationship:

$$K^* = \frac{E^*}{3(1 - 2\nu^*)}$$

$$G^* = \frac{E^*}{2(1 + \nu^*)}$$

Notice that errors in the measured quantities are magnified in the calculated quantities, especially in K* as $|\nu^*|$ approaches 0.5. Therefore, it is

essential to minimize systematic errors. We have avoided some of the possible systematic errors in temperature and frequency by measuring simultaneously E* and \)*, the basic techniques for which have been described in a previous paper.[25] Since our last paper we have refined the technique and automated the testing system. The details of this system are given elsewhere[27] and are only described in brief here.

Dog-bone shaped specimens were cut from as-cast epoxy sheets into ASTM D638 Type I specimens with a thickness of approximately 6mm. The material was isotropic in the plane. These specimens were tested in an automated high response servo-hydraulic testing machine[27] (Instron model 1350) in load control with constant mean load, i.e., equal amplitude tension and compression, and with constant strain amplitude of 0.1%. The latter is essential for obtaining values of Poisson's ratio that are not affected by changing strain amplitude as the specimen compliance changes with temperature. The compression half of the test cycle is feasible because the strain is quite small, and the specimen is quite thick and has been carefully aligned. For the purpose of these tests only the fixed frequency of 1 Hz was used. The temperature of the specimen was monitored with a surface-mounted thin-film type platinum resistance thermometer. This thermometer was insulated from the surroundings by several layers of PTFE tape. The initial values of E* and \)* were measured three to four times at room temperature by shifting the clip-on extensometers around to ensure good alignment, previous experience having indicated the necessity for such a procedure.[25] These initial values were then used to calculate the average at room temperature, and the final results were adjusted accordingly. The specimens were cooled down from room temperature in approximately 10°C steps with 10-15 minutes between each step. The viscoelastic

behavior was monitored throughout the cooling process. This rather slow cooling process is necessary because volumetric thermal expansion and contraction are time-dependent processes, and thermal contraction is especially slow. Thus, the commonly used procedure of cooling as rapidly as possible, usually by enveloping the specimen with cold N_2 gas or liquid and then taking data during heat-up, can produce substantial errors in the initial heat-up portion. Even the slow-cool procedure followed here is not immune to this problem, since the contraction relaxation times involved are orders of magnitude longer than practical laboratory time scale. In these tests the specimens were cooled to approximately -140°C from room temperature in just over three hours. The temperature was then kept constant at the minimum point for between 30 to 60 minutes with the viscoelastic behavior monitored at approximately 10 minute intervals. When it became clear that the measured quantities were changing so slowly as to be unresolvable, then the heat-up run was begun. The heat-up run was performed in 5°C steps, with about 10 minutes total allowed for each step. The temperature was measured before and after each actual series of data taking, and was found to be constant to better than 0.5°. At a given temperature the specimen was cyclically loaded for ten cycles, and data were obtained on the following ten cycles. The change in length of the specimen at each temperature was also recorded. Thus, linear thermal expansivity could be calculated.

8.2 Results and Discussion

Results were obtained only on three resins: DER667/DDS, DER661/DDS, and DER332/DDS. The resins with epoxide equivalent weights intermediate between DER667 and DER661 were not tested because little significant variation was expected. These results are presented in Figure 8-1 to Figure 8-5. Figures

8-1 and 8-2 contain the experimentally obtained results on Young's moduli |E*| and their associated loss tangents and Poisson's ratios |\)*| and their associated phase angles, respectively. Figures 8-3 and 8-4 contain the calculated results on the shear moduli |G*| and their associated loss tangents, and the bulk moduli |K*| and their associated loss tangents, respectively. Finally, Figure 8-5 contains the results on the thermal expansion of the three resins. Since the shear and bulk moduli are of primary concern, their behavior will be discussed first.

The trends caused by increasing cross-link density are quite obvious in the shear modulus. The glass transition temperatures are shifted systematically higher, in agreement with DSC and dynamic torsional measurements in the T_g region. The sub-T_g shear moduli also increase with cross-link density. This trend is intuitively obvious. The presence of the low temperature relaxation peaks lowers |G*| by about a factor of two. This enhancement of shear compliance by the activation of supposedly local segmental mobility is impressive, considering the fact that the maximum tanδ is only about 0.1. The low temperature loss peak (at -72, -67, and -61°C) shifts systematically to higher temperatures with increasing cross-link density. They also decrease slightly in amplitude, and become broader. In DER332/DDS the width of this peak suggests that the maximum at -61°C is actually composed of two peaks. In addition, there is a minor peak (in DER332/DDS) at 59°C. There also appears to be a still lower temperature peak (<-120°C) in all three resins.

The magnitudes of the bulk moduli (Figure 8-4 a-c) of the three resins exhibit an opposite trend from those of the shear moduli. The bulk moduli actually decrease slightly with increasing cross-link density. Since bulk modulus is the inverse of compressibility, we surmise that the higher cross-

link density actually produces a less closely packed structure, hence increasing compressibility. The bulk moduli are also reduced by the occurrence of the relaxations, albeit not to the same extent that the shear moduli are. The error in the calculated bulk loss tends to be relatively large[25], mostly because of possible systematic errors in the phase angle of \)*. We estimate the systematic error in tan (δ_K) to be as much as $\pm 1 \times 10^{-2}$. Given this magnitude of uncertainty, the amplitude of the bulk losses can be considered to be about the same. However, the shape and location of the bulk loss peaks are relatively immune to systematic errors. Thus, it can be ascertained that the bulk loss peaks occur generally at somewhat higher temperatures than their shear counterparts, and that they are also shifted to higher temperatures with increasing cross-linking. The latter shift is larger than that for the shear peaks. These observations can be interpreted in the following manner. Bulk relaxations necessarily involve highly correlated motional processes and are affected by how strongly a relaxing species is coupled to its surroundings. For the bulk effect to be so significant as to reduce the bulk modulus by some 40%, the relaxing molecular species must involve backbone moieties capable of intermolecular motion. Its effect on thermal expansion (Figure 8-5), i.e., the onset of the motion causing a rapid increase in the volume, is further evidence that the motion is strongly intermolecular.[28] The fact that the increasing cross-link density shifts the bulk relaxation peak to systematically higher temperatures can be interpreted to mean that the intermolcular mobility is being gradually reduced. This interpretation might appear intuitively obvious but for the fact that various other reseachers have offered widely disparate interpretations on the nature of these peaks.[17,20,29,30] Some of these interpretations will be addressed in a later section.

For the purpose of the present discussion, suffice it to say that whatever the nature and origin of these relaxation processes, they are being progressively restricted by increasing the cross-link density. This restriction is observed in both the bulk and shear components. How this might affect the toughness of the resin is discussed in this section. For the discussion to be meaningful, it is necessary to define toughness. The terms "fracture toughness" and "ductility" as used by various researchers in the polymer community both carry different connotations. In the present context, fracture toughness is a measure of the total energy dissipated in propagating a sharp crack through a specimen sufficiently thick to satisfy the plane strain condition, and ductility is a measure of the amount of plastic (non-recoverable) strain the material can sustain before fracture occurs. Measurements of ductility are generally carried out under states of stress where the shear component is dominant, whereas measurements of fracture toughness are carried out under states of stress where the hydrostatic tensile component is dominant. Under the latter state of stress, inherent flaws in the material can act as nucleation centers for the formation of voids, which can then develop into crazes or cracks. Thus, a given material can be both ductile and brittle depending on the state of stress. Generally speaking, shear stress leads to yielding and plastic flow, whereas hydrostatic tension leads to dilatation, void formation and brittle fracture. Thus, the brittle and ductile behavior are relatable to the bulk and shear compliance and dissipation. Specifically, shear yield is due to the accumulation of distortional energy, as evidenced by the wide-applicability of the von Mises plastic yield criterion in polymers, and voiding is due to the build-up of bulk energy. Therefore, at any given temperature and time scale, whether a material shear yields or voids depends on the relative rates of shear and bulk energy build-up, dissipation, and the

critical values for yielding and void formation. It can be shown that the relative rates of shear and bulk energy build-up for a given stress state is uniquely determined by the value of the Poisson's ratio.[31] As ν approaches 0.5, the bulk strain energy for any stress state not equal to pure hydrostatic tension is extremely small compared to shear strain energy. This is the reason why materials with ν approximately 0.5 are rarely found to fracture brittlely.

Now that it is clear that ν is an index of the relative rates of accumulation of bulk and shear energies, the deformation behavior of the epoxies in this study can perhaps be better understood. The behavior of the ν^* for the three different resins is shown in Figure 8-2. At all temperatures, the Poisson's ratio increases with increasing molecular weight between cross-links. Furthermore, there is clearly an increase in $|\nu^*|$ associated with each of the low temperature β relaxations. This increase shifts to higher temperatures with increasing cross-link density. Following the reasoning outlined in the last paragraph, then, at any given temperature, the higher the cross-link density, the more the tendency toward brittle fracture. Now it may be argued that this trend is, in any case, intuitively clear. A more critical test may perhaps be an experiment to locate ductile-to-brittle transition temperatures, which is beyond the scope of the present investigation. Still, the results on ν are consistent with the fact that the plane strain fracture toughness of the unmodified epoxies is nearly independent of the cross-link density, since in this case the controlling factor is the rapid build-up of bulk strain energy during the test; but, when rubber-modified, the toughness increases with decreasing cross-link density, since the bulk-strain energy is dissipated by the cavitation of the rubber and subsequent void growth, leaving the built-up

shear strain energy, which increases with \), to cause extensive formation of shear bands. To put it another way, the Poisson's ratio determines the intrinsic manner that strain energy is partitioned between dilatative and shear modes. In plane strain fracture, most of the strain energy is already dilatative, so the small differences in \) do not produce significant differences in the toughness. However, with the incorporation of the rubber particles, the intrinsic ability of the matrix to deform in the shear mode is unleashed.

We now briefly address the question concerning the nature and the origin of the low temperature relaxation peaks. This peak has been variously assigned to the motion of the hydroxyether group[12,20] , the BPA unit[29] , the combination of hydroxyether and unspecified backbone motion[17,30] , and so on. Some of these assignments are based on comparisons with polymers with similar molecular moieties.[29] Others are based on modifications of the curing reaction[17,30] , degree of cure[17] , epoxide equivalent weights[20] , and substitutions with monoepoxide.[30] In one instance[20] the trend for the peak temperature with respect to the cross-link density is opposite to the findings in this work. The cause for this discrepancy is unclear. We note here that the accuracy of dynamic mechanical measurements can be adversely affected by cooling and heating too rapidly and by using variable frequency. These negative factors have largely been avoided in the present investigation. As for the interpretation of dynamic-mechanical spectra, it is widely assumed that not only do various molecular moieties possess individual relaxation peaks, in much the same way as, say, infrared spectroscopy, but also that these peaks are additive. We should like to point out that these assumptions are frequently not correct for the simple reason that molecular motions in the solid

are almost always strongly coupled to their surroundings. That this is true is manifest in the fact that these relaxations are detectable by mechanical spectroscopy and that they affect the compressibility as well as the thermal expansion coefficient. The result of the strong coupling between the motion of a part of the polymer molecule and its surroundings is that the incorporation of various modifications to the polymer is usually not simply an additive effect but that it actually changes the structure of the polymer glass and the entire relaxation spectrum. Thus, for example, if the cross-link density is reduced by some means, the coupling between the relaxation species and their surroundings is expected to be lessened, and the relaxation peak accordingly shifts to lower temperature or shorter times. All these changes can occur without changing the identity of the relaxing species. It is unnecessary to postulate the appearance of new chemical species, as one would be wont to in interpreting IR spectra.

The true identity of the relaxing species can be determined more unambiguously by incorporating substitutions on the benzene rings, which is beyond the scope of the present investigation. Our best estimate is that the motion involves the bisphenol as well as the hydroxyether groups, and that the range of the motion extends over several BPA-hydroxyether units.

(a)

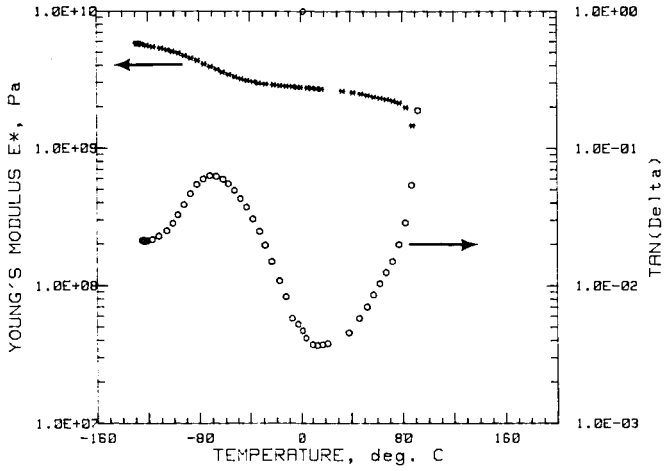

(b)

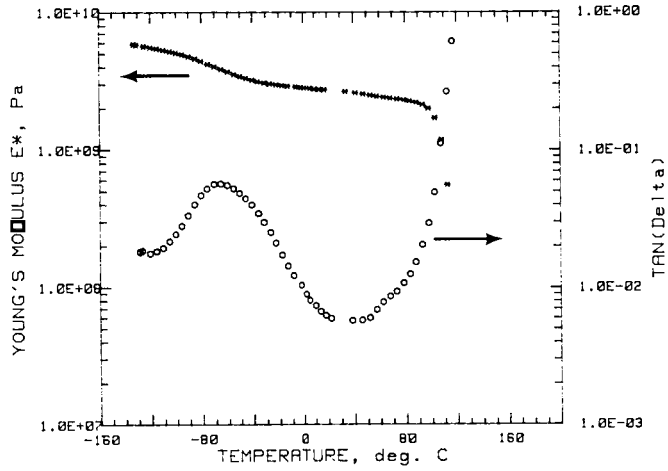

(c)

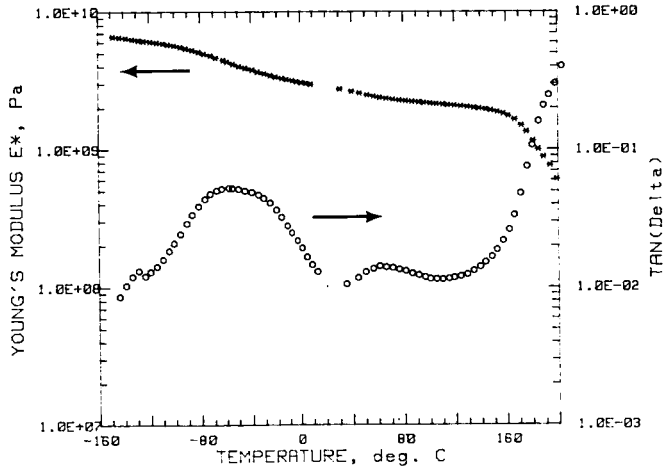

Figure 8-1. Dynamic Young's modulus at 1 Hz (a) DER667/DDS, (b) DER661/DDS, and (c) DER332/DDS.

(a)

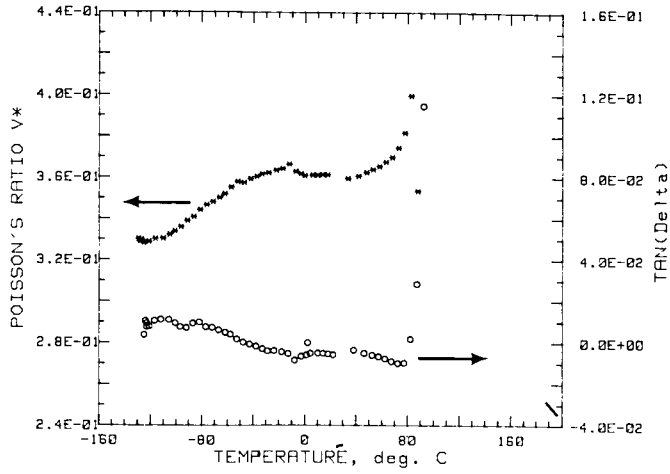

(b)

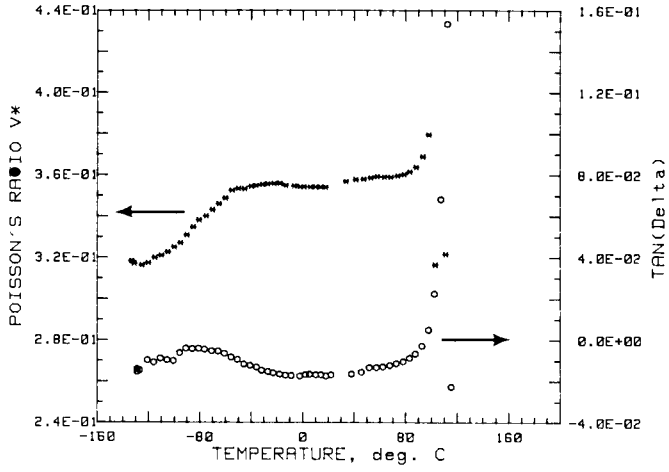

(c)

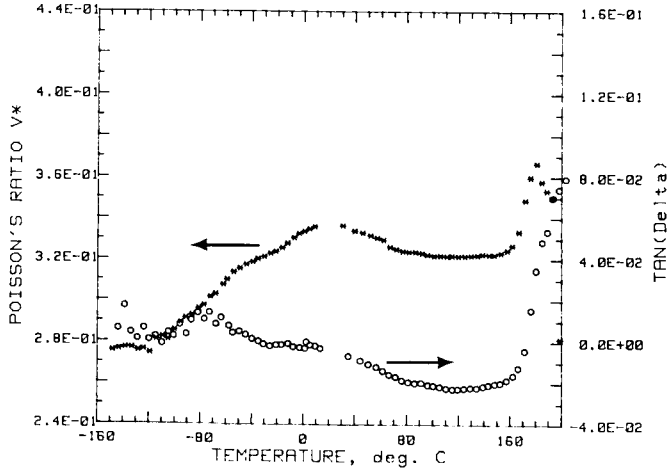

Figure 8-2. Dynamic Poisson's ratio at 1 Hz (a) DER667/DDS, (b) DER661/DDS, and (c) DER332/DDS.

(a)

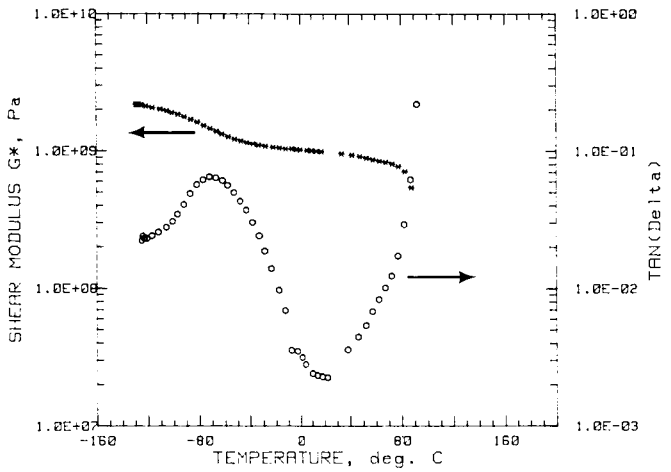

(b)

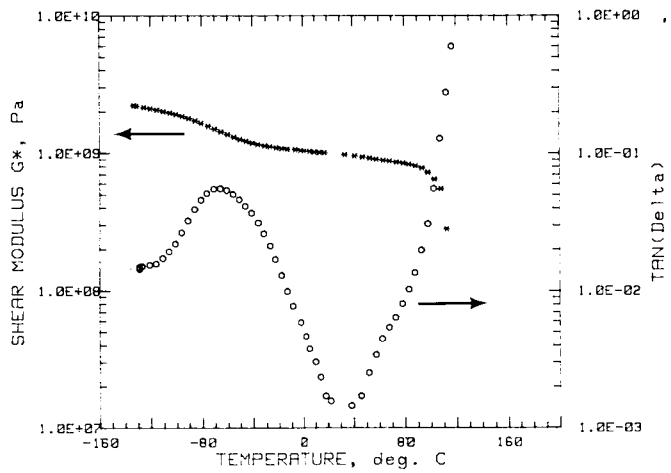

(c)

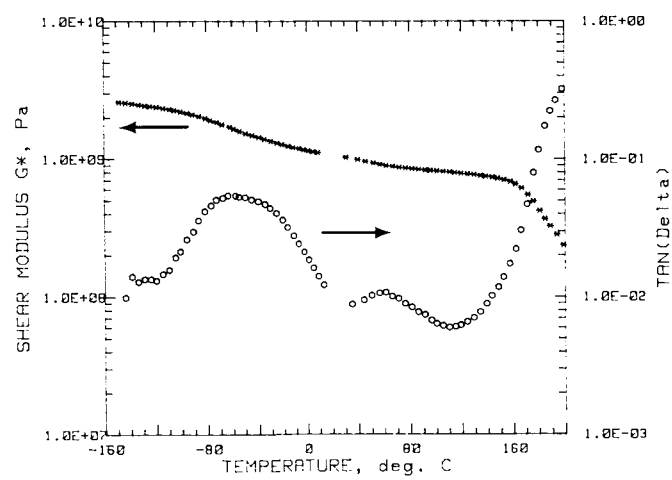

Figure 8-3. Dynamic shear modulus at 1 Hz calculated from E* and \)* measurements. (a) DER667/DDS, (b) DER661/DDS and (c) DER332/DDS.

(a)

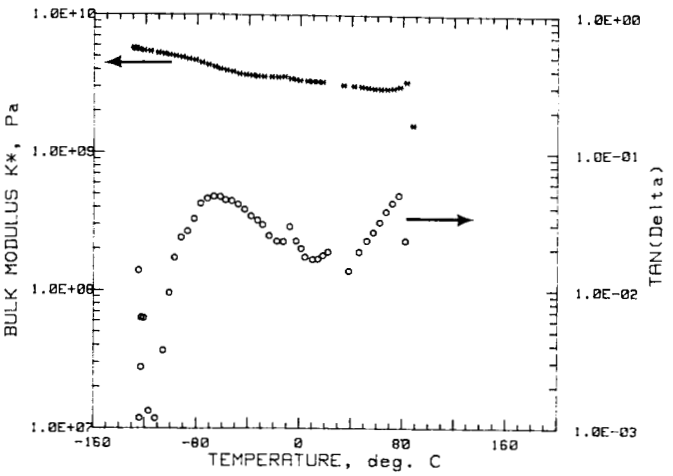

(b)

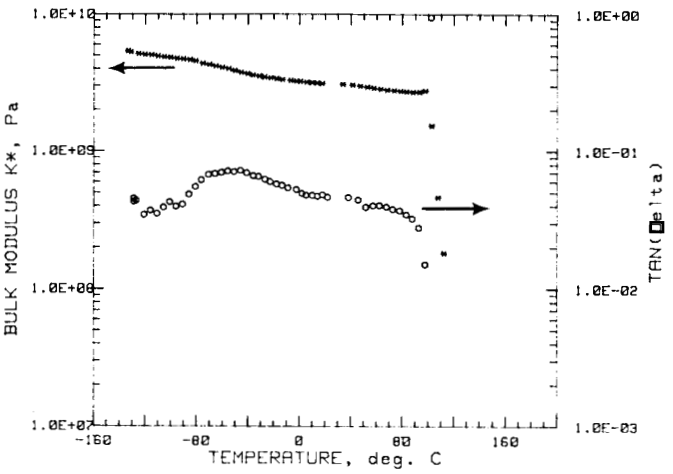

(c)

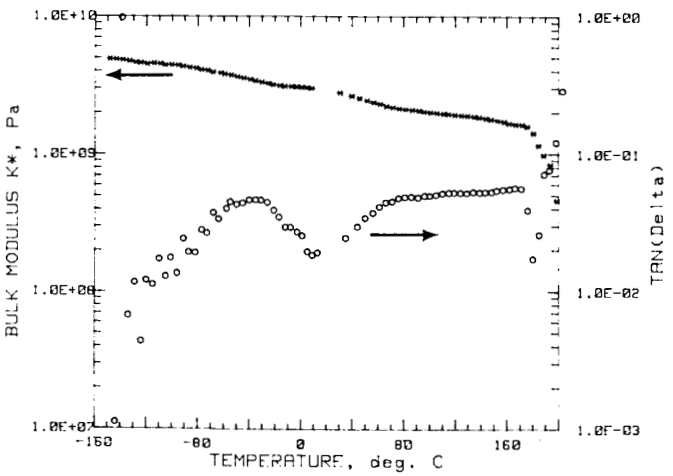

Figure 8-4. Dynamic bulk modulus at 1 Hz calculated from E* and \)* measurements (a) DER667/DDS, (b) DER661/DDS, and (c) DER332/DDS.

(a)

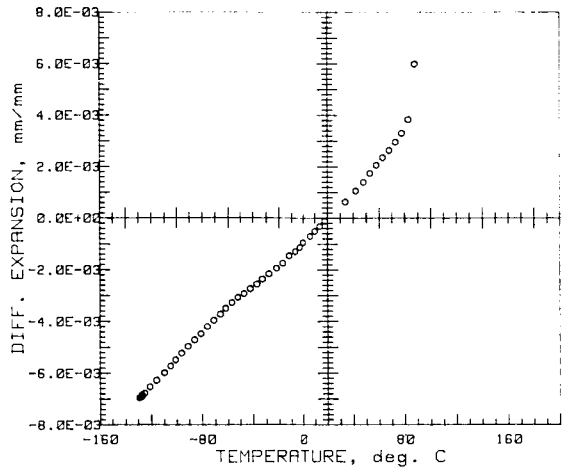

(b)

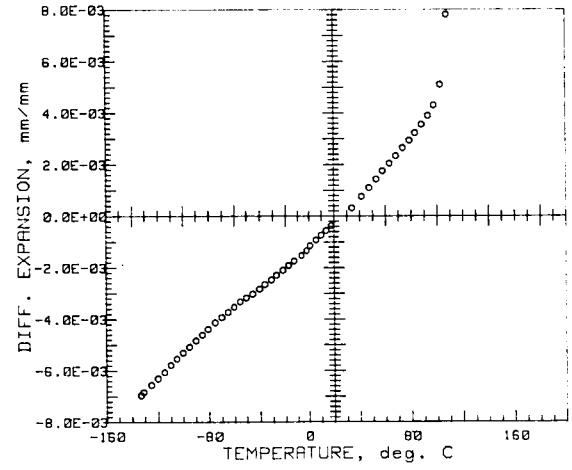

(c)

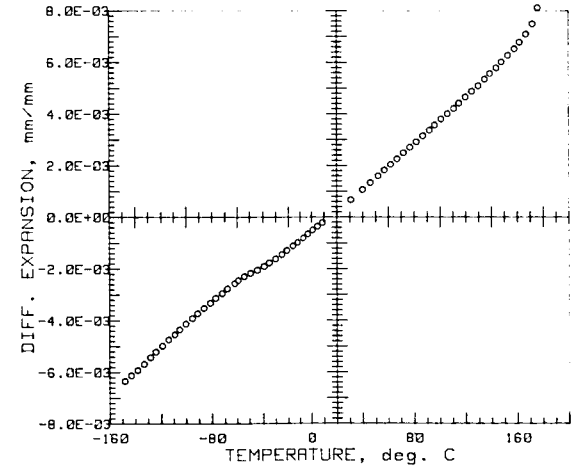

Figure 8-5. Differential linear thermal expansion referenced to room temperature. Time between temperature steps is 8-10 min. (a) DER667/DDS, (b) DER661/DDS, and (c) DER332/DDS.

9. CONCLUSIONS

In our previous investigation (Part1)[1] , we deduced that toughness enhancement by elastomer modification was principally due to two energy dissipation mechanisms occurring at the crack tip. The first mechanism dissipates bulk strain energy via cavitation of the rubber particles. The second mechanism dissipates shear strain energy by enhancing the formation of shear bands by the voided rubber particles. In this investigation, it was found that a large decrease in cross-link density of neat DGEBA epoxies cured with DDS produced only a modest increase in fracture toughness, and simple elastomeric modification of these epoxies did not guarantee enhanced toughness. However, the toughenability was found to be a strong function of the inherent matrix ductility, which is a function of cross-link density. The micromechanical mechanisms, voiding and enhanced shear band formation, are again the energy dissipation processes.

It can be argued that the increase in toughenability originates from increased ductility which is due to a lowering of the glass-transition temperature. However, high glass transition temperatures do not necessarily correspond to brittleness; in fact, many high T_g polymers are very ductile when tested in uniaxial tension at room temperature. We contend that as long as the matrix is ductile, then it can be toughened by the addition of a rubbery phase.

The results of the dynamic bulk and shear relaxation studies show that the shear modulus increases while the bulk modulus decreases with cross-link density. Low temperature relaxation peaks also exist in the bulk mode. The small relative shifts in the positions of the bulk and shear peaks with cross-

link density result in turn in shifts of low-to-high Poisson's ratio transitions. This latter shift may explain why shear mode deformation becomes progressively more difficult as the cross-link density increases.

10. ACKNOWLEDGEMENTS

The authors wish to thank Dr. N. Johnston of NASA-Langley, the Contract Monitor of this work, for his encouragement and patience.

The authors also wish to acknowledge the assistance of the following scientists at General Electric Corporate Research and Development: Mr. J. Grande for performing the optical microscopy work; Dr. M.T. Takemori, Dr. D.S. Matsumoto, Mr. T.A. Morelli and Ms. L.M. Carapellucci for stimulating discussions; Dr. A.R. Shultz and Mrs. A.L. Young for their assistance with the DSC T_g measurements; Dr. E.A. Williams for the ^{13}C NMR work; and Drs. S.Y. Hobbs and P.C. Juliano for their support.

REFERENCES

1. A.F. Yee and R.A. Pearson, "Toughening Mechanism in Elastomer-Modified Epoxy Resins - Part 1", NASA Contractor Report 3718 (August 1983).

2. W.D. Bascom, R.L. Cottington, R.L. Jones, and P. Peyser, "The Fracture of Epoxy and Elastomer Modified Epoxy Polymers in Bulk and As Adhesives", J. Appl. Polym. Sci., 19, 2425 (1975).

3. W.D. Bascom and R.L. Cottington, "Effect of Temperature on the Adhesive Fracture Behavior of an Elastomer" J. Adhesion, 7, 333 (1976).

4. C. Meeks, "Fracture and Mechanical Properties of Epoxy Resins and Rubber-Modified Epoxy Resins", Polymer, 15, 675 (1974).

5. T.D. Chang, and J.O. Brittain, "Studies of Epoxy Resins Systems Part D: Fracture Toughness of an Epoxy Resin: A Study of the Effect of Cross-Linking and Sub-T_g Annealing" Poly. Eng. and Sci., 22, 1228 (1982).

6. J.N. Sultan, R.C. Laible, and F.J. McGarry "Microstructure of Two-Phase Polymers", Appl. Poly. Symp., 16, 127 (1971).

7. B.W. Cherry and K.W. Thompson, "The Fracture of Highly Cross-Linked Polymers", J. Mater. Sci., 16, 1913 (1981).

8. J.M. Scott, G.M. Wells and D.C. Phillips, "Low Temperature Crack Propagation in an Epoxide Resin", J. Mater. Sci., 15, 1436 (1980).

9. J.D. Ferry, "Viscoelastic Properties of Polymers", 3rd ed., John Wiley Sons, Inc., New York, 1980.

10. E. Plati and J.G. Williams, "The Determination of the Fracture Parameters for Polymers in Impact", Poly. Eng. Sci., 15, 470 (1975).

11. P.E. Reed, "Impact Performance Of Polymers" in Developments in Polymer Fracture-1, Applied Science Publishers, pp 121-152 (1977).

12. C.B. Bucknall, "Toughened Plastics", Applied Science, London, 1977.

13. H. Lee and K. Neville, "Handbook of Epoxy Resins", McGraw-Hill Book Co., New York, 1967.

14. L.E. Nielson, "Effects of Cross-Linking On The Glass Transitions", J. Macromol. Sci., Rev. Macromol. Chem., C3(1), 77 (1969).

15. L. Banks and B. Ellis, "The Glass Transition Temperatures of Highly Cross-Linked Epoxy Networks: Cured Epoxy Resins", Polymer, 23, 1466 (1982).

16. H.F. Rietsch, "Statistical Thermodynamic Treatment of Glass Transition for Cross-Linked Polymers of Varying Functionality", Macromolecules, 11, 477 (1978).

17. M. Ochi, M. Okazaki and M. Shimbo, "Mechanical Relaxation Mechanism of Epoxide Resins Cured With Alphatic Diamines", J. Poly. Sci.: Poly. Phys. Ed., 20, 689 (1982).

18. J.P. Bell, "Structure of a Typical Amine-Cured Epoxy Resin", J. Poly. Sci. Part A-2, 6, 417 (1970).

19. L. Buckley and D. Roylance, "Kinetics of a Sterically Hindered Amine-Cured Epoxy System", Poly. Eng. Sci., 22, 166 (1982).

20. T. Takahama and P.H. Geil, "Dynamic Mechanical Properties of Epoxy Resins", J. Poly. Sci.: Poly. Letters Ed., 20, 453 (1982).

21. D. Katz and A.V. Tobolsky, "Rubber Elasticity in a Highly Cross-Linked System", Polymer, 4, 417 (1963).

22. C.K. Riew, E.H. Rowe and A.R. Siebert, in "Advances in Chemistry Series, No. 154, Toughness and Brittleness of Plastics", American Chemical Society, 326 (1976).

23. C.T. Hooley, D.R. Moore, M. Whale and M.J. Williams, "Fracture Toughness of Rubber Modified PMMA", Plastics and Rubber Processing and Applications, 1, 345 (1981).

24. M.A. Maxwell and A.F. Yee, "The Effect of Strain Rate on the Toughening Mechanisms of Rubber-Modified Plastics", Poly. Eng. and Sci., 21, 205 (1981).

25. A.F. Yee and M.T. Takemori, "Dynamic Bulk and Shear Relaxation in Glassy Polymers. I. Experimental Techniques and Results on PMMA". J. Poly. Sci.: Poly. Phys. Ed., 20, 205 (1982).

26. A.F. Yee, "Dynamic Bulk and Shear Relaxations in Solid Polymers: Relationship to Deformation Behavior". Proc. 5th Int. Conf. Deformation, Yield and Fracture Of Polymers, 1982, Cambridge.

27. A.F. Yee, "Dynamic Mechanical Analysis of Practical Plastic Specimens Using an Automated Servo-hydralic Tester", Proc. SPE ANTEC (Chicago), 29, 538 (1983).

28. J.M. Roe and R. Simha, "Thermal Expansivity and Relaxational Behavior of Amorphous Polymers at Low Temperatures", Inter. J. Poly. Mater., 3, 193 (1974).

29. E. Cuddihy and J. Moacanin, "Dynamic Mechanical Properties of Epoxides β-Transition Mechanism", p. 96 in "Epoxy Resins", R.F. Gould, ed., #92 in Adv. Chem. Ser., ACS, 1970.

30. J.G. Williams, "The Beta Relaxation in Epoxy Resin-Based Networks", J. App. Poly. Sci., 23, 3433 (1979).

31. J.G. Williams, "Stress Analysis of Polymers", J. Wiley and Sons, New York, 1973, p. 49.

32. A.J. Kinloch and J.G. Williams, "Crack Blunting Mechanisms in Polymers", J. Mater. Sci., 15, 978 (1980).

1. Report No.	2. Government Accession No.	3. Recipient's Catalog No.
NASA CR-3852		

4. Title and Subtitle	5. Report Date
TOUGHENING MECHANISM IN ELASTOMER-MODIFIED EPOXY RESINS—PART 2	December 1984
	6. Performing Organization Code
7. Author(s)	8. Performing Organization Report No.
A. F. Yee and R. A. Pearson	84-SRD-041
	10. Work Unit No.
9. Performing Organization Name and Address General Electric Company Corporate R&D Center P.O. Box 8 Schenectady, NY 12301	11. Contract or Grant No. NAS1-16132
	13. Type of Report and Period Covered Contractor Report July 1, 1982-Aug. 30, 1983
12. Sponsoring Agency Name and Address National Aeronautics and Space Administration Washington, DC 20546	14. Sponsoring Agency Code

15. Supplementary Notes

Langley Technical Monitor: Norman J. Johnston
Final Report

16. Abstract

The role of matrix ductility on the toughenability and toughening mechanism of elastomer-modified DGEBA epoxies was investigated. Matrix ductility was varied by using epoxide resins of varying epoxide monomer molecular weights. These epoxide resins were cured using 4,4′ diaminodiphenyl sulfone (DDS) and, in some cases, modified with 10% HYCAR^{R} CTBN 1300X8. Fracture toughness values for the neat epoxies were found to be almost independent on the monomer molecular weight of the epoxide resin used. However, it was found that the fracture toughness of the elastomer-modified epoxies was very dependent upon the epoxide monomer molecular weight. Tensile dilatometry indicated that the toughening mechanism, when present, is similar to the mechanism found for the piperidine cured epoxies in Part 1.[1] SEM and OM corroborate this finding.

Dynamic mechanical studies were conducted to shed light on the toughenability of the epoxies. The time-dependent small strain behavior of these epoxies were separated into their bulk and shear components. The bulk component is related to brittle fracture, whereas the shear component is related to yielding. It can be shown that the rates of shear and bulk strain energy buildup for a given stress are uniquely determined by the values of Poisson's ratio, ν. It was found that ν^* increases as the monomer molecular weight of the epoxide resin used increases. This increase in ν^* can be associated with the low temperature β relaxation. The effect of increasing cross-link density is to shift the β relaxation to higher temperatures and to decrease the magnitude of the β relaxation. Thus, increasing cross-link density decreases ν^* and increases the tendency towards brittle fracture. The nature and origin of the low temperature relaxation peaks is briefly addressed.

17. Key Words (Suggested by Author(s))	18. Distribution Statement
Epoxy Rubber-modified epoxy Impact Fracture toughness Epoxy mechanical properties Polymer mechanical properties Dynamic mechanical properties Cross-link density	Unclassified - Unlimited Subject Category 27

19. Security Classif. (of this report)	20. Security Classif. (of this page)	21. No. of Pages	22. Price
Unclassified	Unclassified	56	A04

For sale by the National Technical Information Service, Springfield, Virginia 22161

NASA-Langley, 1984